THE JOURNAL OF PHYSICAL CHEMISTRY B

ARTICLE

pubs.acs.org/JPCB

# Structure and Dynamics of a Dizinc Metalloprotein: Effect of Charge Transfer and Polarization

Yong L. Li,[†] Ye Mei,[*,‡,§] Da W. Zhang,[∥] Dai Q. Xie,[⊥] and John Z. H. Zhang[*,‡,§,#]

[†]Key Laboratory of Mesoscopic Chemistry of MOE, School of Chemistry and Chemical Engineering, Nanjing University, Nanjing 210093, China

[‡]State Key Laboratory of Precision Spectroscopy, East China Normal University, Shanghai 200062, China

[§]Institute of Theoretical and Computational Science, East China Normal University, Shanghai 200062, China

[∥]Division of Chemistry and Biological Chemistry, School of Physical and Mathematical Sciences, Nanyang Technological University, Singapore 637371

[⊥]School of Chemistry and Chemical Engineering, Nanjing University, Nanjing 210093, China

[#]Department of Chemistry, New York University, New York 10003, United States

Supporting Information

**ABSTRACT:** Structures and dynamics of a recently designed dizinc metalloprotein (DFsc) (*J. Mol. Biol.* **2003**, *334*, 1101) are studied by molecular dynamics simulation using a dynamically adapted polarized force field derived from fragment quantum calculation for protein in solvent. To properly describe the effect of charge transfer and polarization in the present approach, quantum chemistry calculation of the zinc-binding group is periodically performed (on-the-fly) to update the atomic charges of the zinc-binding group during the MD simulation. Comparison of the present result with those obtained from simulations under standard AMBER force field reveals that charge transfer and polarization are critical to maintaining the correct asymmetric metal coordination in the DFsc. Detailed analysis of the result also shows that dynamic fluctuation of the zinc-binding group facilitates solvent interaction with the zinc ions. In particular, the dynamic fluctuation of the zinc−zinc distance is shown to be an important feature of the catalytic function of the di-ion zinc-binding group. Our study demonstrates that the dynamically adapted polarization approach is computationally practical and can be used to study other metalloprotein systems.

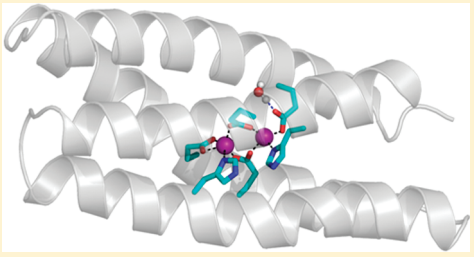

## INTRODUCTION

About one-third of all known proteins have metal ions as their cofactors. These metalloproteins carry out various functions in cells such as enzyme catalysis, transport and storage, signal transduction, etc.[1] Metals may possess more than one redox and spin states, and their coordination numbers may vary in different proteins and in different functional stages. Therefore, understanding the structure and function of metalloprotein can provide much insight into enzyme catalysis and protein function in general.

The *de novo* designed dizinc metalloprotein (DFsc, shown in the top graphic of Figure 1) is a single-chain protein[2] which shares a common metal motif with many metalloproteins, including bacterioferritin, ribonucleiotide reductase, hydroxylase, and the acyl carrier protein $\Delta^9$ desaturase.[3] The purpose of designing the DFsc is to obtain insight on its catalytic mechanism.[3] In the DFsc, the di-ion site is housed asymmetrically within a four-helix bundle consisting of four carboxylate and two histidine ligands.[3] In previous studies, the DFsc displayed similar catalytic function as methane monooxygenase;[4,5] that is, its catalytic mechanism involves ligand binding to the active site as the first step, followed by an $O_2$ insertion into the middle of two metal ions to create an intermediate state containing mixed 4- and 5-valence metal ions.[6] The two zinc ions in the zinc binding group (ZBG) (here, it is a simple reference to represent the zinc center in the DFsc; see the bottom graphic of Figure 1) are asymmetrically coordinated and serve as the catalytic center. While the specific coordination numbers for the two zinc ions are still unclear, there is evidence for other zinc analogs showing the asymmetry of two metal ions.[7−10]

In the equilibrium structure of the ZBG, two zinc ions are surrounded by four glutamic acids (GLU or E), and two of them serve as bridges between the zinc ions through coordination bonds formed between their carboxylate oxygen atoms and zinc ions. Together with two zinc ions, they form an eight-membered ring. The other two GLUs interact, respectively, with each of the zinc ions and form coordination bonds with them, in either monodentate or bidentate mode. In an earlier structural refinement study by Calhoun et al.,[7] it was found that the coordination of the glutamic acid E11 to ZN2 is monodentate whereas the

**Received:** April 15, 2011
**Revised:** July 18, 2011
**Published:** July 18, 2011

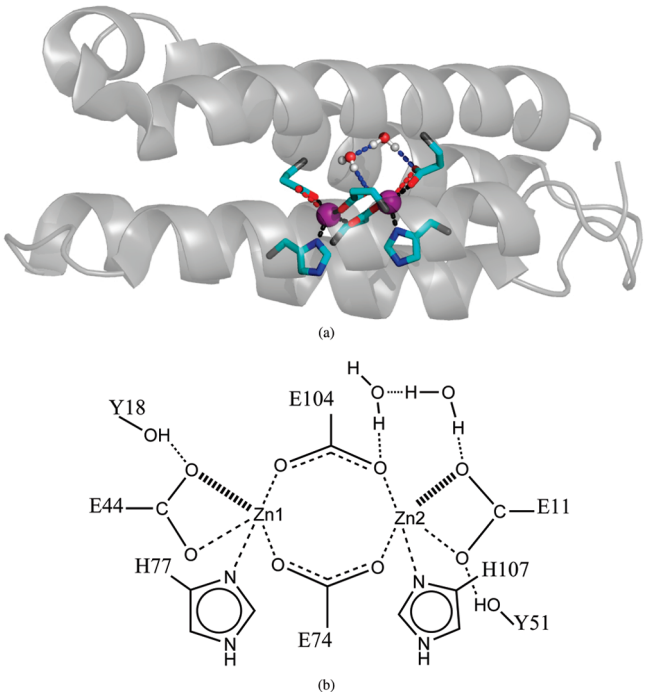


**Figure 1.** (top) NMR structure of DFsc (PDB code: 2HZ8). Zinc binding group (ZBG) and hydrogen bonded (H bonded) waters are shown explicitly. (bottom) NMR structure of the zinc binding group. Both the first and the second coordination shell are shown. Residues are capped by ACE and NME at the terminals. There are 168 atoms in total. The ZBG for the APPC calculation does not include two tyrosines and two waters.

coordination of E44 to ZN1 is bidentate. Also, each HIS forms one coordination bond to each zinc ion from one side of the eight-membered ring, leaving the opposite side exposed to the solvent accessible channel to be available for interaction with exogenous ligands.[3]

Molecular dynamics (MD) studies of proteins can provide much insight into the structure and dynamics of proteins at the atomic level. Although a nonbonded model is suitable for studying coordination dynamics, previous studies showed that the structure of a metal protein may distort severely in the standard force field with an integer charge assigned to the metal.[11,12] Thus, reparametrization of the metal cluster is needed in the nonbonded model to correctly reproduce the structure of the metal cluster embedded in the protein, which is needed for the accurate prediction of binding affinity,[13] refinement of NMR structures,[7] and other equilibrium properties.[14−16] It is known that, without charge transfer, the nonbonded model tends to give the highest coordination numbers to the metal.[15,17−19] Lim and co-workers carried out systematic studies of metals, especially divalent metals, in protein and in aqueous solution. They proposed a new force field that includes charge transfer and a local polarization effect.[1,20−22] More sophisticated approaches such as *ab initio* molecular dynamics or quantum mechanical/molecular mechanics hybrid methods are able to provide a more accurate description of the dynamics and have been successfully applied to the structural refinement of biomolecules.[7,23−26] However, these methods are computationally expensive and, therefore, difficult to apply to long time dynamics studies of metalloproteins.

In this work, we develop a theoretical approach that includes charge transfer and polarization for dynamics studies of metalloproteins. The method is based on a recently developed polarized protein-specific charge (PPC)[27] but with modification to properly treat the metal-binding group in the metalloprotein. The PPC is restrictively fitted to the electrostatic potential (RESP) generated from the fragment quantum chemistry calculation[28] coupled with the Poisson−Boltzmann (PB) continuum solvation model for a given protein structure.[27] The PPC has been applied to a series of benchmark protein systems and has been shown to give better agreement with experimental results than do standard nonpolarizable force fields for properties such as equilibrium structure, binding free energy, p$K_a$ shifts, NMR order parameters, etc.[29−34] It was demonstrated that the incorrectly distorted structure of the metalloprotein can be restored in the MD simulation when the PPC was employed.[35] However, in the standard PPC application, the PPC is derived on the basis of a single protein structure, usually the native structure. For simulations with a large conformational change, a charge update is needed to reflect the conformation-dependence of atomic charges. In the current work, we employ the dynamically adapted charge scheme APPC (adaptive polarized protein-specific charge).

The main purpose of the present study is to address the following questions. First, whether MD simulation using the APPC is suitable for studying zinc-binding metalloprotein. Second, whether simulation using the APPC reveals the correct catalytic characteristics of the DFsc and helps understand the fluctuations of the ZBG in the DFsc. For comparison, MD simulations using various versions of the standard AMBER force fields (AMBER94, AMBER99, AMBER99SB, and AMBER03) are also performed. All MD simulations are carried out at room temperature and in explicit water.

## THEORY AND COMPUTATION

The initial structure of the DFsc is taken from the deposited structure in the protein data bank (PDB entry 2HZ8, the top graphic of Figure 1). The system is soaked in a periodic TIP3P water box with the smallest distance between the protein and cell boundary set to 12 Å. The system is relaxed in 10 000 steps with a 100 kcal/mol·Å$^2$ constraint on the protein, followed by further minimization without any constraints until convergence is reached. The energy minimized protein is then heated to 300 K within 200 ps with a 10 kcal/mol·Å$^2$ constraint on the protein. The temperature is regulated using Langevin dynamics with the collision frequency set to 1 ps$^{-1}$. All the covalent bonds involving hydrogen atoms are fixed by applying the SHAKE algorithm.[36] An integration time step of 2 fs is used in the MD simulation.

The initial atomic charges are calculated from the published structure based on the PPC scheme. A detailed description of the PPC fitting can be found in an earlier work,[27] and here, we only give a brief description. In the PPC scheme, the protein is decomposed into amino acid-based fragments that are properly capped to saturate the covalent bonds and mimic their chemical environment. Standard QM calculations are carried out for each fragment using Gaussian03[37] at the B3LYP/6-31G* level. In the QM calculation of each fragment, the other residues are taken into account as background charges, and the solvation effect is included by solving the PB (Poisson−Boltzmann) equation using the Delphi program.[38] The atomic charges are fitted using the RESP method.[39] The process is iterated until the fitted atomic charges are converged within a preset limit.[27]

In the present approach, the ZBG is treated as a special fragment, which includes two zinc ions and their coordinated ligands.

So, the charge redistribution within the ZBG is properly included from the quantum chemistry calculation of the fragment. Further, during the MD simulation, the quantum calculation of the ZBG fragment is performed periodically to update its atomic charges. However, atomic charges of other fragments are kept at their initial values. Test results show that an updating period of 100 ps is a suitable choice. Because the ZBG contains two zinc cations and six residues (E11, E44, E74, E104, H77, and H107) with a total of 168 atoms, the RESP fitting of atomic charges could encounter numerical difficulties.[40] The experimental vdW radius of 1.40 Å for the zinc atom is shown to give better solvation free energy values in the PB solvation model[11] and is adopted in our APPC simulations instead of the default value 1.10 Å used in AMBER10.

For the purpose of comparison, standard MD simulations are also performed using various versions of AMBER force fields, including AMBER94,[41] AMBER99,[42] AMBER99SB,[43] and AMBER03.[44,45] It is useful to point out that when a radius of 1.40 Å is used in the AMBER99SB simulation, the protein backbone deviates a lot from the crystal structure during MD simulation (see the Supporting Information). Thus, in these simulations, the vdW radii of the zinc atoms are set to the default value of 1.10 Å,[46] and the partial charge of the zinc is set to 2.0*e* following the standard procedure. Comparisons between these results and those obtained from the APPC simulation provide explicit information on the effect of charge transfer and polarization on the structure and dynamics of the DFsc. All the simulations are carried out using the Sander module in the AMBER 10 package.[47]

## RESULTS AND DISCUSSION

**Validation of Simulated Structure of the DFsc.** The structure of the DFsc is generally stabilized after about 6 ns, and the simulation is carried out for a total of 12 ns. The rmsd (root-mean-square deviation) from the initial structure is about 1.75 Å under the APPC. For comparison, the rmsd under the standard AMBER force fields is somewhat larger (around 2.0 Å). It should also be noted that a recent MD study by Peraro et al. based on a modified AMBER94 force field[18] gave a much larger rmsd (>3 Å).

The solvent accessible surface (SAS) of the DFsc provides an access channel of the active site to the surface. The simulation shows that the proper channel allowing the contact of zinc ions with solvent is well maintained. This channel plays a crucial role in the function of the DFsc but is ill-recognized by normal NMR experiments.[7] However, MD simulations employing the APPC give a correct representation of this channel. The volume of this channel is measured to be 278 Å$^3$, using VOIDOO software,[48] which is slightly larger than that of the initial structure (236 Å$^3$). The NOE violations of the simulated structures with the initial structure (PDB code 2HZ8) are also analyzed using the experimental NMR constraints (in BioMagResBank under accession number 7247[7]).[49] The NOE violation of the final structure is found to be comparable to that of the initial structure. More detailed results are given in Table 3 of the Supporting Information.

The above analysis indicates that the simulated protein structure under the APPC is well characterized and should be a reasonable representation of the correct structure of the DFsc.

**Coordination of Zinc Ions.** The initial structure of the ZBG in Figure 1 and Figure 2a shows that the two zinc ions in the active site are asymmetrically positioned and have different binding geometries. Also, two water molecules form a hydrogen bond (H bond) network with E11 and E104.[7] Although the 4−5 coordination feature of the Fe-substituted DFsc is well-recognized from circular dichroism/magnetic circular dichroism, specifically which ion is 4-coordinated and which is 5-coordinated is still unclear in the DFsc.[7] For comparison, the simulated structure of the ZBG under the APPC is shown (Figure 2b) together with the structure obtained under the AMBER99SB force field (Figure 2c). As shown in Figure 2b, the simulated structure under the APPC maintains a 4−5 coordination pattern and has a H bonded water molecule. However, the two zinc ions undergo a coordination rearrangement; namely, the Zn1 changes from 5-coordination to 4-coordination while Zn2 changes from 4-coordination to 5-coordination. This rearrangement results in a monodentate E44 and a bidentate E11. The specific values of these bond lengths are listed in Table 1, and their time evolutions are plotted in Figure 3.

From Table 1, the E44@OE1−Zn1 distance of 2.43 Å is just on the fringe of a normal Zn−O coordination bond (2.1−2.4 Å).[20] In addition, this bond length fluctuates a lot, as can be seen from

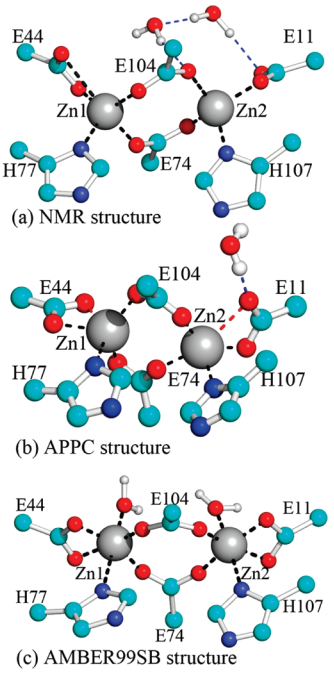


**Figure 2.** Final structures of the ZBG under different simulations. The side chains of the residues are truncated, and the NMR structure is taken from ref 7. Color code: silver, Zn; cyan, C; red, O; blue, N; white, H; black dashed line, coordination bond; blue dashed line, H bond; red dashed line, weakened or broken coordination bond.

**Table 1. Calculated Average Distances between Zinc and Oxygen/Nitrogen Atoms of the ZBG (in Å) Compared with NMR Experimental Values[a]**

| ZN1 | APPC | NMR[18] | ZN2 | APPC | NMR[18] |
|---|---|---|---|---|---|
| E44@OE1 | 2.43 ± 0.40 | 2.10 | E11@OE1 | 2.24 ± 0.22 | 2.14 |
| E44@OE2 | 2.08 ± 0.23 | 2.07 | E11@OE2 | 2.11 ± 0.34 | 2.11 |
| E74@OE1 | 2.15 ± 0.15 | 2.22 | E74@OE2 | 2.04 ± 0.06 | 2.25 |
| H77@ND1 | 2.46 ± 0.28 | 2.03 | H107@ND1 | 2.50 ± 0.64 | 2.09 |
| E104@OE2 | 2.04 ± 0.06 | 2.13 | E104@OE1 | 2.07 ± 0.12 | 2.17 |

[a] The labels of residues are given in Figure 1, and the names of the atoms are adopted from PDB convention.

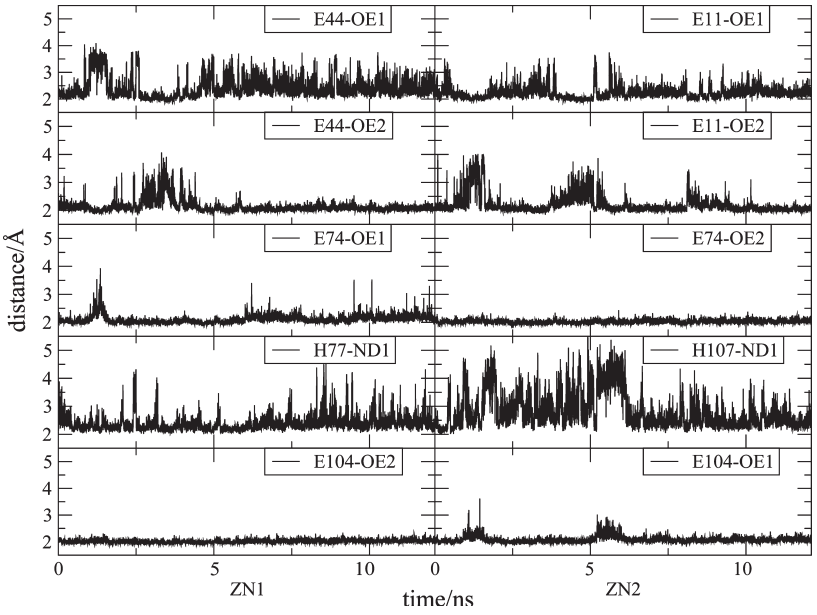


**Figure 3.** Time-dependence of coordination bond lengths of the ZBG under the APPC simulation. There are large fluctuations before 6 ns.

the rmsd values in Table 1 and Figure 3. Here, the symbol E44@OE1 denotes the carboxylate oxygen atom OE1 in the 44th residue and so forth. The analysis of the distance E44@OE1−Zn1 shows that this distance can be recognized as a coordination bond only within about 60.0% of the simulation time. This phenomenon is actually due to the perturbing hydrogen bonds. Our analysis shows that there is a stable (93% occupancy) H bond between E44@OE1 and Y18@OH−HH (shown in the bottom graphic of Figure 1) which perturbs and weakens the E44@OE1−Zn1 coordination bond. For comparison, because there is no H bond perturbation, the coordination bond E44@OE2−Zn1 remains stable (see Figure 3). The effect of hydrogen bonding on the stability of a coordination bond was recognized by Ryde et al.,[50] who demonstrated that hydrogen bonds play a non-negligible role in the zinc−carboxylate binding mode.

It is also interesting to examine the other two coordination bonds, E11@OE1−Zn2 and E11@OE2−Zn2 (see the bottom graphic in Figure 1); both bond lengths show large fluctuations. The former (with an average bond length of 2.24 Å) is weakened by the WAT−E1@OE1 hydrogen bond while the latter is weakened by the hydrogen bond Y51−E11@OE2. However, from Table 1, their bond lengths are in the normal range of coordination bonds. The reason why the coordination bond E11@OE1−Zn2 is stronger than its analog E44@OE1−Zn1 is likely due to the smaller mass of the water molecule relative to that of tyrosine. Moreover, the occupancy of the WAT−E11@OE1 hydrogen bond is only 76%, which is weaker than that for Y18−E44@OE1 (93% occupancy). Also, the coordination bond E11@OE2−Zn2 is only slightly weakened by the hydroxyl group of Y51 (Table 1), as shown by the smaller fluctuation of the bond length (see Figure 3). The detailed plots of distances of H bond vs time are shown in Figure 5 in the Supporting Information.

In comparison, the simulation results under various versions of AMBER force fields (AMBER94, AMBER99, AMBER99SB, and AMBER03) all give similar but incorrect structures of the ZBG. Using AMBER99SB as an example, nearly all neighboring oxygen atoms, including those of water molecules, coordinate to the zinc ions as shown in Figure 2c and result in the highest coordination mode for the ZBG (hexa-coordinated). This phenomenon occurs very early in the simulation. The overestimation of the coordination number of the zinc ion was observed earlier by Kollman et al.,[11] who recognized that this phenomenon would happen if no charge transfer is allowed within the ZBG. In addition, the coordination bonds between the zinc ions and imidazole rings are permanently broken in AMBER94 and AMBER03 force fields (shown in the Supporting Information). This phenomenon was also observed by other groups.[20,51] From the hard−soft acid−base (HSAB) theory,[52] the use of the AMBER force field with the partial charge 2.0 for Zn(II) produces an artificially hard (Lewis) acid, which tends to make the maximum number of coordination bonds with the oxygen of hard base carboxylic acid, as shown in Figure 2c.

**Dynamics of Water and Coordination Bonds of the ZBG.** In addition to the previous analysis on the dynamic fluctuations of the distances E11@OE1−Zn1 and E44@OE1−Zn2, two additional coordination bonds H77@ND1−Zn1 and H107@ND1−Zn2 are also interesting to discuss. As shown in Figure 3, these two coordination bonds are also experiencing large dynamic fluctuations during MD simulation, similar to those of E11@OE1−Zn1 and E44@OE1−Zn2. With the assistance of the time-dependent trajectory (see Supporting Information), the underlying cause of dynamic fluctuation of these coordination bonds is due to the dynamic motion of water molecules inside the solvent accessible channel. As much as one knows, the DFsc is a simple mimic of a wide variety of non-heme iron enzymes.[2] In those real enzymes, the solvent accessible channels are protected by other subunits (see review in ref 53), and they only open when a catalytic reaction takes place. When the channel is open, the water molecules move immediately into the reaction site at the bottom of the channel and play a critical role in metal catalysis.[6] However, in the DFsc, this channel is always open to water. Thus, during the pre-equilibrium process, the interaction between the water and zinc ions in the DFsc could provide some characteristic dynamic features of the early stage of catalysis in real non-heme iron enzymes and is therefore meaningful to study here.

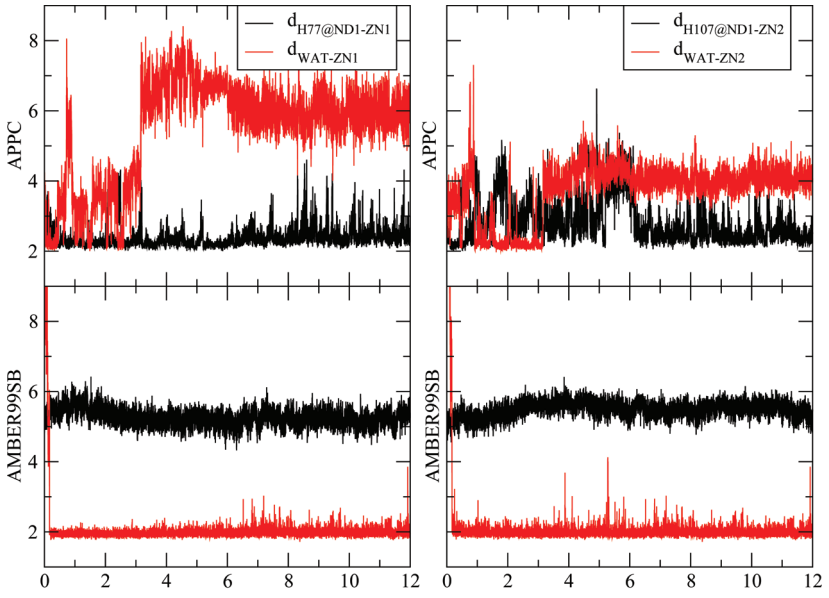


**Figure 4.** Time-dependent distances between ND1s and zinc ions. For comparison, the closest water−zinc distances are also displayed. The upper panel is from the APPC simulation while the lower panel is from the AMBER99SB simulation. Results from other AMBER force fields are essentially the same as that from the AMBER99SB simulation.

When the channel opens, the water molecules enter through the channel and approach the zinc ions. Our analysis shows that when water molecules approach the zinc ions, they can temporarily form coordination bonds with both zinc ions. However, these water molecules do not stay there for long and leave the zinc within 3 ns. However, there is one water molecule left behind to form a H bond with E11@OE1, as shown in Figure 2b. Once the waters leave, the excess oxygen atom of E11@OE1 is pushed off Zn2, which then re-forms a coordination bond with the imidazole ring. After the ZBG reaches its equilibrium state in ca. 6 ns, one of the water molecules near Zn1 leaves the channel while the other water leaves Zn2 but still stays in the ZBG by forming a H bond with E11@OE1. The water polarizes Zn2, and this results in the imidazole ring of H107 being pushed away from Zn2.

The time evolution of the water−zinc distance ($d_{WAT-ZN}$) and the HIS@ND1s−zinc distance ($d_{ND1-ZN}$) are plotted in Figure 4. Because there are seven waters and two zinc ions that participate in the water−zinc interaction and five of the seven waters can move close to the zinc ions, we plot the nearest distance between a water and Zn1 or Zn2 at each snapshot in Figure 4. Detailed water−zinc ion distances are shown in Figure 4 in the Supporting Information. Clearly, there is a correlation between these two distances. When $d_{WAT-ZN}$ is small, $d_{ND1-ZN}$ becomes large and vice versa. To investigate the correlated motion, we calculate the dynamics cross correlation (DCC). The DCC for a specified pair of atoms $i$ and $j$ is defined by[54]

$$C_{ij} = [\langle (r_i - \langle r_i \rangle)\,(r_j - \langle r_j \rangle)\rangle]/\sqrt{\langle r_i^2 \rangle \langle r_j^2 \rangle} \quad (1)$$

where the symbol $\langle\ \rangle$ represents the time average over the trajectory. The delayed DCC is defined by[55]

$$C_{ij}(d) = 1/N\,\{\sum_k [(r_i(k) - \langle r_i \rangle)\,(r_j(k+d) - \langle r_j \rangle)]\}/\sqrt{\langle r_i^2 \rangle \langle r_j^2 \rangle} \quad (2)$$

**Table 2. Time-Averaged Distance between the Two Zinc Atoms**[a]

| method | value (Å) |
|---|---|
| APPC | 3.68 ± 0.50 |
| AMBER99SB | 4.27 ± 0.31 |
| Peraro2007[18] | 3.60 ± 0.20 |
| Peraro2008[7] | 4.16 |
| expr[18] | 3.75 |

[a] The APPC and AMBER99SB values are from the current work, and the Peraro2007 value is from MD simulation by Peraro et al.[18] The Peraro2008 value is from MD simulation followed by QM/MM by Peraro et al.[7] The experimental value is from ref 18.

where $d$ denotes the time delay and $k$ runs from 1 to $N$, assuming there are $N$ discrete $r_i$ values. A positive value denotes time advance, and a negative value denotes time lag. Here, the values for $k + d > N$ or $k + d < 0$ are simply ignored.

The calculated dynamic cross correlation (DCC)[54] between $d_{WAT-ZN1}$ and $d_{H77@ND1-ZN1}$ is −0.178, and that between $d_{WAT-ZN2}$ and $d_{H107@ND1-ZN2}$ is −0.113. The negative correlation between them is consistent with the previous analysis of their dynamic events. In contrast, during simulations under AMBER force fields, the waters float in the solvent accessible channel at the very beginning, and once they arrive at the bottom of the channel, they ligate to the zincs tightly and form strong coordination bonds to the zinc ions (as could be seen in Figure 4). This makes harder zinc ions, which prefer the highest coordination to oxygen atoms.

**Dynamic Fluctuation of Zn−Zn Distance.** As shown in Table 2, the average Zn−Zn distance in the APPC simulation is about 3.68 Å, in excellent agreement with the experimentally measured value of 3.75 Å. The current result is also in good agreement with an early study by Peraro et al., who used modified charges of the AMBER94 force field.[18] In comparison, the

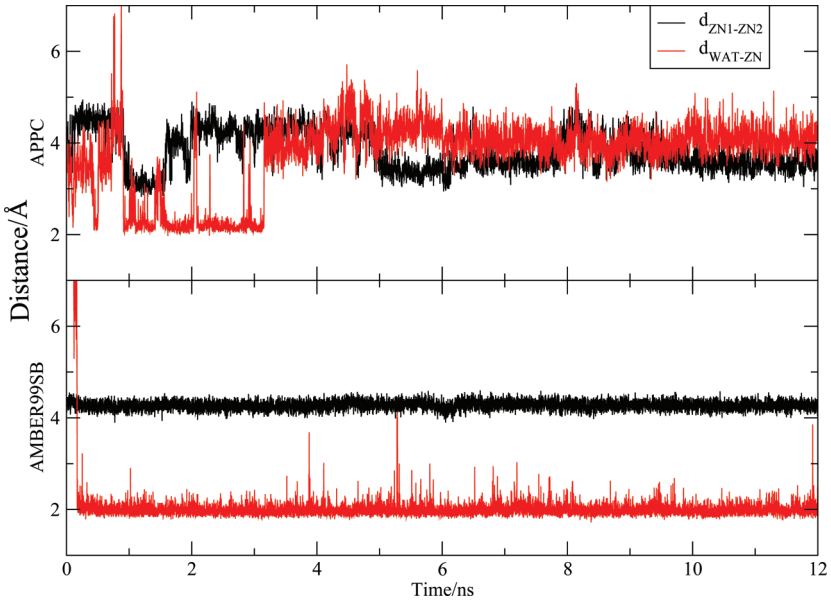


**Figure 5.** Time-dependence of the zinc−zinc distance and the closest water−zinc distance. The upper panel is from the APPC simulation while the lower panel is from the AMBER99SB simulation. Results from other AMBER force fields are essentially the same as that from AMBER99SB.

simulation results from various AMBER force fields give overestimated Zn−Zn distances. For example, simulation with AMBER99SB gives an average distance of 4.27 Å, about 0.5 Å larger than the experimental value (see Table 2). Other AMBER force fields give very similar values (they are listed in the Supporting Information, Table 1). The large value of $d_{ZN-ZN}$ was also reported in another work,[7] which used QM/MM for structural refinement but used the standard AMBER94 force field for the MD simulation.

It is important to note that the Zn−Zn distance fluctuates a lot during the MD simulation under the APPC. As shown in Table 2, the rmsd of the Zn−Zn distance reached 0.5 Å, which is much larger than those obtained under the AMBER force fields. To understand the nature of this fluctuation, the Zn−Zn distance $d_{ZN-ZN}$ is plotted in Figure 5. During the first 1 ns, the waters moved quickly and randomly in the solvent channel. Between 1 and 5 ns, two water molecules formed two coordination bonds (each with one of the zinc ions). When the waters moved away from the two zinc ions, they dragged the bonded zinc ions with them. The DCCs between the Zn−Zn distance ($d_{ZN-ZN}$) and water−zinc distances ($d_{WAT-ZN1}$ and $d_{WAT-ZN2}$) are shown in Table 3. From the table, the positive correlations (0.26 and 0.41) of $d_{WAT-ZN1}-d_{ZN-ZN}$ and $d_{WAT-ZN2}-d_{ZN-ZN}$ support this analysis. However, after 5 ns, only one water remains in the channel, and its coordination bond with the zinc is broken. Then, the water forms an H bond with E11@OE1 and remains there. When this water moves toward two zinc ions, it pushes them away from each other, and when it leaves, the two zinc ions return toward each other. Thus, it shows a negative correlation between $d_{WAT-ZN1orZN2}$ and $d_{ZN-ZN}$ (from Table 3, −0.08 and −0.13). Because the mass of the zinc ion is about three times greater than that of water, there is a small time delay between the motions of water and zinc ions. To support this analysis, the delayed DCC is calculated. The maximum DCC between $d_{ZN-ZN}$ and $d_{WAT-ZN1}$ is obtained by delayed times 108 and 270 ps, respectively, as given in Table 3. This delayed effect is also observed in Figure 5. The above discussion on the mechanism of the DCC is illustrated

**Table 3. Dynamic Cross Correlation (DCC) between $d_{WAT-ZN}$ and $d_{ZN1-ZN2}$ within 12 ns[a]**

| type | 1.0−5 ns | 5−12 ns | maximum delayed correlation (5−12 ns) |
|---|---|---|---|
| $d_{WAT-ZN1}$ | 0.26 | −0.08 | −0.24 (−108 ps) |
| $d_{WAT-ZN2}$ | 0.41 | −0.13 | −0.23 (−270 ps) |

[a] $d_{WAT-ZN}$ denotes the distance between the O atom of the water and the zinc ion. The notation of atoms is given in Figure 2b. Before the system reaches its equilibrium (<5 ns), the relevant distances are positively correlated. After that, they become negatively correlated. This correlation relation suggests that the fluctuation of the zinc−zinc distance is closely correlated to the motion of water toward and away from the zinc ions.

schematically in Figure 6. Thus, the large fluctuation of Zn−Zn distance is closely correlated with the motion of water moving toward and away from the zinc ions. In summary, the above analysis suggests that the large fluctuation of zinc−zinc distance results from the dynamic motion water.

Although the interesting phenomenon under the APPC simulation, that is, the relatively large fluctuation of the Zn−Zn distance but overall stability of the protein backbone, may appear contradictory, it is consistent with the inherent nature of enzymes that show stable structures but have active reaction centers, as it is understood that protein function and stability are often the result of opposite requirements.[3] In the native form of this di-ion coordination core of methane monooxygenase, the reaction mechanism contains a similar process of water−zinc interaction. With the help of a solvent molecule, an $O_2$ molecule inserts into the middle of two iron ions and forms a mixed-valence intermediate.[6] From previous experiments, the iron-coordinated DFsc could catalyze the same type of reaction, and the zinc-substituted form of this coordination can perform a similar function.[4,5]

In comparison, the Zn−Zn distance under the AMBER force field is relatively stable. A water forms a coordination bond with

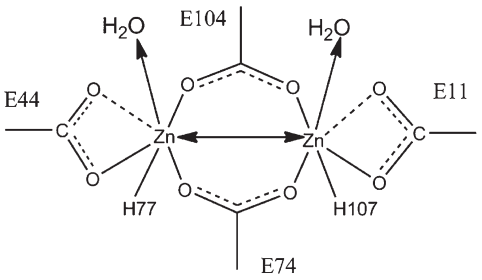


Scheme 1: When waters ligate to Zn, they show positive correlation with Zn-Zn distance. The arrows denote directions of motion.

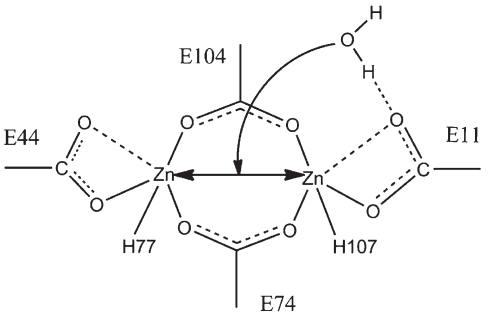


Scheme 2: When water forms hydrogen bond with E11, it shows negative correlation with Zn-Zn distance. The arrows denote directions of motion.

**Figure 6.** Schematic diagram showing correlated dynamic motion between $d_{WAT-ZN}$ and $d_{ZN1-ZN2}$.

**Table 4. Partial Atomic Charges of the First Coordination Shell of Residues of the ZBG from Different Charge Schemes**[a]

| res[b] | atom | PPC | Peraro2008[7] | AMBER03 |
|---|---|---|---|---|
| ZN | ZN1 | 1.19 | 1.35 | 2.00 |
| ZN | ZN2 | 1.36 | 1.35 | 2.00 |
| H77 | ND1 | −0.54 | −0.65 | −0.54 |
| H107 | ND1 | −0.67 | −0.65 | −0.54 |
| E11 | OE1 | −0.65 | −0.74 | −0.82 |
| E11 | OE2 | −0.86 | −0.84 | −0.82 |
| E44 | OE1 | −0.70 | −0.74 | −0.82 |
| E44 | OE2 | −0.76 | −0.84 | −0.82 |
| E74 | OE1 | −0.53 | −0.74 | −0.82 |
| E74 | OE2 | −0.72 | −0.84 | −0.82 |
| E104 | OE1 | −0.69 | −0.74 | −0.82 |
| E104 | OE2 | −0.88 | −0.84 | −0.82 |

[a] Residues are shown in the bottom graphic of Figure 1, and the names of the atoms are from the PDB convention. The PPC charges shown are obtained at 10 ns, and their values at other simulation times are provided in Table 2 of the Supporting Information. [b] Abbreviation for residue.

the zinc ion, and it stays there permanently. As shown in Table 2, the Zn−Zn distance is overestimated by about 0.5 Å. The reason for this overestimation of Zn−Zn distance under the AMBER force field is most likely due to overcharged Zn(II) in AMBER, which would make two zinc ions repel each other.

**Effective Partial Charges of the ZBG.** To understand the charge transfer and polarization effect in the ZBG, atomic charges of atoms directly linked to the zinc ions are calculated near the end of the simulation time (10 ns) and are shown in Table 4. From the table, the APPC charges are similar to those obtained by the QM/MM calculation of ref 7. This indicates that charge-transfer and polarization are correctly represented in both approaches. It is useful to note that the atomic charges of the two zinc ions are not symmetric under the APPC scheme, unlike those given in the QM/MM calculation of ref 7, which enforced the symmetry. Different partial charges of the zinc ions are indicative of the asymmetric coordination nature of the two zinc ions.

It is also important to note that these partial charges are dynamic, meaning that they are dynamically fluctuating as a function of time. In contrast, MD simulations based on charges fitted from a single structure of the ZBG are incapable of reproducing the above thermodynamic structure. Instead, they produce structures with the incorrect coordination modes for the zinc ions.

It was pointed out by Lim and co-workers[20] that Zn(II) ion prefers the bidentate coordination mode in water or the first ligand shell is perturbed by the second ligand shell but prefers the monodentate coordination mode when only side chains are around it. From Table 4, the charges of the two oxygen atoms of E11 and E44 are different, indicating that they are in different chemical environments, confirming Lim's conclusion. This charge differentiation cannot be represented by a nonpolarizable force field that gives symmetric charges to the two oxygen atoms and, therefore, leads to bidentate coordinated zinc.

## CONCLUSION

Multiple MD simulations are carried out to study the structure and dynamics of the dizinc metalloprotein DFsc using the APPC, which includes charge transfer and polarization, and various versions of the AMBER force fields for comparison. In the APPC simulation, the correct structure of the ZBG has been maintained, especially the characteristic 4−5 coordination states of the two zinc ions. Because the atomic charges of the ZBG are updated on-the-fly in the APPC, it correctly takes the dynamic charge transfer and polarization of the ZBG into account in the MD simulation, and thus, it can correctly describe the coordination number switching of metal ions, which is essential for zinc binding in natural proteins.[51] The APPC MD simulation also revealed the in-and-out motions of waters through the ligand binding channel. This dynamic effect is critical in metal ion catalysis of non-heme proteins[53] whose catalytic functions are mimicked by the DFsc. There are already experiments reporting oxidation reactions catalyzed by the DFsc, in which the zinc ions are replaced by Fe(II) ions[4], and its two-chain analogue DF3.[5] In these reported reactions, the ligand binding to the metal atom is essential to the catalytic reaction. Thus, the in-and-out motion of the waters and the interaction between the waters and zinc ions observed in this work may help shed light on the realistic dynamic mechanism of the DFsc catalysis.

Current MD studies based on the APPC scheme, which includes dynamic charge transfer and polarization through updating of atomic charges for the metal binding group, give the correct coordination dynamics of the ZBG and the flexible dynamics of the metal binding group. To be more attractive, application of this approach is quite straightforward and requires no parameter-refitting of the force field before the MD simulation.

These features make the APPC approach attractive for application to other metal-containing systems to gain insight on the dynamic mechanism of catalysis and the ligand binding process of metalloproteins, such as matrix metalloproteinase (MMP),[56] zinc finger,[57] etc.

For comparison, simulations under the standard AMBER force fields failed to maintain the correct structure of the ZBG, gave incorrect coordination number of the zinc ions, and were unable to describe the in-and-out motion of water through the ligand binding channel.

## ■ ASSOCIATED CONTENT

**Supporting Information.** Three additional tables and five additional figures providing additional data and information from our calculations for further detailed analysis and comparison. This material is available free of charge via the Internet at http://pubs.acs.org.

## ■ AUTHOR INFORMATION

**Corresponding Author**

*E-mail: ymei@phy.ecnu.edu.cn; john.zhang@nyu.edu.

## ■ ACKNOWLEDGMENT

Y.M. is supported by National Natural Science Foundation of China (Grant No. 20803034). J.Z.H.Z. acknowledges financial support from National Natural Science Foundation of China (Grant Nos. 10974054 and 20933002) and Shanghai PuJiang program (09PJ1404000). This work is partly supported by the State Key Laboratory of Precision Spectroscopy of East China Normal University. We also thank the High Performance Computer Center of East China Normal University and Shanghai Supercomputer Center for support of CPU time.

## ■ REFERENCES

(1) Sakharov, D. V.; Lim, C. *J. Am. Chem. Soc.* **2005**, *127*, 4921–4929.
(2) Calhoun, J. R.; Kono, H.; Lahr, S.; Wang, W.; DeGrado, W. F.; Saven, J. G. *J. Mol. Biol.* **2003**, *334*, 1101–1115.
(3) Calhoun, J. R.; Nastri, F.; Maglio, O.; Pavone, V.; Lombardi, A.; DeGrado, W. F. *Pept. Sci.* **2005**, *80*, 264–278.
(4) Calhoun, J. R.; Bell, C. B.; Smith, T. J.; Thamann, T. J.; DeGrado, W. F.; Solomon, E. I. *J. Am. Chem. Soc.* **2008**, *130*, 9188–9189.
(5) Faiella, M.; Andreozzi, C.; de Rosales, R. T. M.; Pavone, V.; Maglio, O.; Nastri, F.; DeGrado, W. F.; Lombardi, A. *Nat. Chem. Biol.* **2009**, *5*, 882–884.
(6) Murray, L. J.; García-Serres, R.; McCormick, M. S.; Davydov, R.; Naik, S. G.; Kim, S.-H.; Hoffman, B. M.; Huynh, B. H.; Lippard, S. J. *Biochemistry* **2007**, *46*, 14795–14809.
(7) Calhoun, J. R.; Liu, W.; Spiegel, K.; Dal Peraro, M.; Klein, M. L.; Valentine, K. G.; Wand, A. J.; DeGrado, W. F. *Structure* **2008**, *16*, 210–215.
(8) Wei, P.-p.; Skulan, A. J.; Wade, H.; DeGrado, W. F.; Solomon, E. I. *J. Am. Chem. Soc.* **2005**, *127*, 16098–16106.
(9) Papoian, G. A.; DeGrado, W. F.; Klein, M. L. *J. Am. Chem. Soc.* **2003**, *125*, 560–569.
(10) Magistrato, A.; DeGrado, W. F.; Laio, A.; Rothlisberger, U.; VandeVondele, J.; Klein, M. L. *J. Phys. Chem. B* **2003**, *107*, 4182–4188.
(11) Donini, O. A. T.; Kollman, P. A. *J. Med. Chem.* **2000**, *43*, 4180–4188.
(12) Tuccinardi, T.; Martinelli, A.; Nuti, E.; Carelli, P.; Balzano, F.; Uccello-Barretta, G.; Murphy, G.; Rossello, A. *Bioorg. Med. Chem.* **2006**, *14*, 4260–4276.
(13) Jain, T.; Jayaram, B. *Proteins: Struct., Funct., Bioinf.* **2007**, *67*, 1167–1178.
(14) Oelschlaeger, P.; Schmid, R. D.; Pleiss, J. *Protein Eng.* **2003**, *16*, 341–350.
(15) Antony, J.; Piquemal, J. P.; Gresh, N. *J. Comput. Chem.* **2005**, *26*, 1131–1147.
(16) Spiegel, K.; Grado, W. F. D.; Klein, M. L. *Proteins: Struct., Funct., Bioinf.* **2006**, *65*, 317–330.
(17) Gresh, N.; Piquemal, J. P.; Krauss, M. *J. Comput. Chem.* **2005**, *26*, 1113–1130.
(18) Peraro, M. D.; Spiegel, K.; Lamoureux, G.; De Vivo, M.; DeGrado, W. F.; Klein, M. L. *J. Struct. Biol.* **2007**, *157*, 444–453.
(19) Johansson, M. P.; Kaila, V. R. I.; Laakkonen, L. *J. Comput. Chem.* **2008**, *29*, 753–767.
(20) Dudev, T.; Lim, C. *Chem. Rev.* **2003**, *103*, 773–787.
(21) Babu, C. S.; Lim, C. *J. Phys. Chem. A* **2006**, *110*, 691–699.
(22) Sakharov, D. V.; Lim, C. *J. Comput. Chem.* **2009**, *30*, 191–202.
(23) Ryde, U. *Dalton Trans.* **2007**, 607–625.
(24) Ryde, U.; Greco, C.; De Gioia, L. *J. Am. Chem. Soc.* **2010**, *132*, 4512–4513.
(25) Wu, E. L.; Wong, K. Y.; Zhang, X.; Han, K. L.; Gao, J. L. *J. Phys. Chem. B* **2009**, *113*, 2477–2485.
(26) Wu, R. B.; Hu, P.; Wang, S. L.; Cao, Z. X.; Zhang, Y. K. *J. Chem. Theory Comput.* **2009**, *6*, 337–343.
(27) Ji, C. G.; Mei, Y.; Zhang, J. Z. H. *Biophys. J.* **2008**, *95*, 1080–1088.
(28) Zhang, D. W.; Zhang, J. Z. H. *J. Chem. Phys.* **2003**, *119*, 3599–3605.
(29) Ji, C. G.; Zhang, J. Z. H. *J. Phys. Chem. B* **2009**, *113*, 16059–16064.
(30) Ji, C. G.; Zhang, J. Z. H. *J. Am. Chem. Soc.* **2008**, *130*, 17129–17133.
(31) Duan, L. L.; Mei, Y.; Zhang, Q. G.; Zhang, J. Z. H. *J. Chem. Phys.* **2009**, *130*, 115102.
(32) Tong, Y.; Ji, C. G.; Mei, Y.; Zhang, J. Z. H. *J. Am. Chem. Soc.* **2009**, *131*, 8636–8641.
(33) Tong, Y.; Mei, Y.; Li, Y. L.; Ji, C. G.; Zhang, J. Z. H. *J. Am. Chem. Soc.* **2010**, *132*, 5137–5142.
(34) Lu, Y. P.; Mei, Y.; Zhang, J. Z. H.; Zhang, D. W. *J. Chem. Phys.* **2010**, *132*, 131101.
(35) Xu, Z. J.; Mei, Y.; Duan, L. L.; Zhang, D. W. *Chem. Phys. Lett.* **2010**, *495*, 151–154.
(36) Ryckaert, J. P.; Ciccotti, G.; Berendsen, H. J. C. *J. Comput. Phys.* **1977**, *23*, 327–341.
(37) Frisch, M. J.; Trucks, G. W.; Schlegel, H. B.; Scuseria, G. E.; Robb, M. A.; Cheeseman, J. R.; Montgomery, J. A., Jr.; Vreven, T.; Kudin, K. N.; Pople, J. A.; et al. *Gaussian 03*, Revision D.01; Gaussian Inc.: Wallingford, CT, 2004.
(38) Rocchia, W.; Sridharan, S.; Nicholls, A.; Alexov, E.; Chiabrera, A.; Honig, B. *J. Comput. Chem.* **2002**, *23*, 128–137.
(39) Bayly, C. I.; Cieplak, P.; Cornell, W. D.; Kollman, P. A. *J. Phys. Chem.* **1993**, *97*, 10269–10280.
(40) Mei, Y.; Zhang, J. Z. H. *J. Theor. Comput. Chem.* **2009**, *8*, 925–942.
(41) Cornell, W. D.; Cieplak, P.; Bayly, C. I.; Gould, I. R.; Merz, K. M.; Ferguson, D. M.; Spellmeyer, D. C.; Fox, T.; Caldwell, J. W.; Kollman, P. A. *J. Am. Chem. Soc.* **1995**, *117*, 5179–5197.
(42) Wang, J. M.; Cieplak, P.; Kollman, P. A. *J. Comput. Chem.* **2000**, *21*, 1049–1074.
(43) Hornak, V.; Abel, R.; Okur, A.; Strockbine, B.; Roitberg, A.; Simmerling, C. *Proteins: Struct., Funct., Bioinf.* **2006**, *65*, 712–725.
(44) Duan, Y.; Wu, C.; Chowdhury, S.; Lee, M. C.; Xiong, G. M.; Zhang, W.; Yang, R.; Cieplak, P.; Luo, R.; Lee, T.; Caldwell, J.; Wang, J. M.; Kollman, P. *J. Comput. Chem.* **2003**, *24*, 1999–2012.
(45) Lee, M. C.; Duan, Y. *Proteins: Struct., Funct., Bioinf.* **2004**, *55*, 620–634.
(46) Hoops, S. C.; Anderson, K. W.; Merz, K. M. *J. Am. Chem. Soc.* **1991**, *113*, 8262–8270.
(47) Case, D. A.; Darden, T. A.; Cheatham, T. E., III; Simmerling, C. L.; Wang, J.; Duke, R. E.; Luo, R.; Crowley, M.; Walker, R. C.; Zhang, W.; Merz, K. M.; Wang, B.; Hayik, S.; Roitberg, A.; Seabra, G.; Kolossváry, I.; Wong, K. F.; Paesani, F.; Vanicek, J.; Wu, X.; Brozell, S. R.; Steinbrecher, T.; Gohlke, H.; Yang, L.; Tan, C.; Mongan, J.;

Hornak, V.; Cui, G.; Mathews, G.; Seetin, M. G.; Sagui, C.; Babin, V.; Kollman, P. A. *AMBER 10*; University of California: San Francisco, 2008.

(48) Kleywegt, G. J.; Jones, T. A. *Acta Crystallogr., Sect. D: Biol. Crystallogr.* **1994**, *50*, 178–185.

(49) Laskowski, R. A.; Rullmann, J. A. C.; MacArthur, M. W.; Kaptein, R.; Thornton, J. M. *J. Biomol. NMR* **1996**, *8*, 477–486.

(50) Ryde, U. *Biophys. J.* **1999**, *77*, 2777–2787.

(51) Stote, R. H.; Karplus, M. *Proteins: Struct., Funct., Genet.* **1995**, *23*, 12–31.

(52) Pearson, R. G. *J. Am. Chem. Soc.* **1963**, *85*, 3533–3539.

(53) Solomon, E. I.; Brunold, T. C.; Davis, M. I.; Kemsley, J. N.; Lee, S.-K.; Lehnert, N.; Neese, F.; Skulan, A. J.; Yang, Y.-S.; Zhou, J. *Chem. Rev.* **1999**, *100*, 235–350.

(54) Hünberger, P. H.; Mark, A. E.; van Gunsteren, W. F. *J. Mol. Biol.* **1995**, *252*, 492–503.

(55) Chatfield, C. *The Analysis of Time Series: An Introduction*, 6th ed.; Chapman & Hall/CRC: Boca Raton, London, New York, Washington, DC, 2003; p 156.

(56) Yu, A. E.; Hewitt, R. E.; Connor, E. W.; Stetler-Stevenson, W. G. *Drugs Aging* **1997**, *11*, 229–244.

(57) Lipscomb, W. N.; Strater, N. *Chem. Rev.* **1996**, *96*, 2375–2434.